Copolymerization of Ethylene with Polar Monomers by Anionic Substitution. Theoretical Study Based on Acrylonitrile and the Brookhart Diimine Catalyst

Miklos J. Szabo,† Natasha M. Galea,† Artur Michalak,‡ Sheng-Yong Yang,† Laurent F. Groux,† Warren E. Piers,† and Tom Ziegler*,†

Department of Chemistry, University of Calgary, University Dr. 2500, Calgary, Alberta, Canada T2N 1N4, and Department of Theoretical Chemistry, Faculty of Chemistry, Jagiellonian University, R. Ingardena 3, 30-060 Cracow, Poland

Received December 10, 2004

Calculations have been carried out on the complexation energy of acrylonitrile and ethylene using derivatives of the cationic N^N Ni(II)−diimine Brookhart complex. For acrylonitrile (CH_2=CHCN) considerations were given to both π binding through the olefinic C=C functionality and σ binding through the NC group. The diimine ring system N^N = $-NR''CR_1$-CR_2NR'' with R″ = 2,6-C_6H_3(*i*-Pr)$_2$ and R_1, R_2 = CH_3 was functionalized by substituting a carbon in the diimine ring by B^- and R_1 or R_2 (or both) by anionic groups (BF_3^-, OBF_3^-, etc.). Substitutions were also carried out at the aryl rings by replacing H or *i*-Pr with anionic groups. The objective has been to find substitutions that would reduce or eliminate the preference for σ complexation of acrylonitrile, a prerequisite for ethylene/acrylonitrile copolymerization.

Introduction

The introduction of polar monomers[1,2] into the polymer chain by coordination copolymerization with ethylene remains a significant challenge. The incorporation of polar monomers is attractive, as it substantially enhances polymer properties such as toughness, adhesion, paintability, printability, and solvent resistance.

Currently the copolymerization of ethylene with polar monomers is carried out by radical polymerization processes, where the ability to control the polymer composition is minimal.[3] Recent studies have shown that late-transition-metal complexes exhibit some promise as polar copolymerization catalysts for oxygen- and nitrogen-containing monomers, whereas early metals[4] are poisoned by the polar groups binding to the metal. Brookhart[5] and co-workers have focused on the copolymerization of ethylene with vinyl ketones and acrylates using both Pd(II) and Ni(II) cationic diimines as catalysts. Other alternatives involve the Ni(II) salicylaldiminato catalyst developed by Grubbs and coworkers[6] and the bidentate P−O nickel system (developed by Keim for the Shell Higher Olefin Process—SHOP) studied by Drent and Keim.[7] Other recent works include experimental studies by Bazan[8] and Peters[9] as well as theoretical investigations by Goddard,[10] Svensson,[11] and Ziegler.[12]

Copolymerization of ethylene with acrylonitrile (AN: CH_2=CHCN) has met with less success than for other polar monomers. The nitrogen-containing monomer can bind to the metal via the polar CN group (σ bond) or the olefinic C=C π bond (Scheme 1). For polymerization of the olefin to take place, the π binding mode should

* To whom correspondence should be addressed. E-mail: ziegler@ucalgary.ca.
† University of Calgary.
‡ Jagiellonian University.

(1) (a) Boffa, L. S.; Novak, B. M. *Chem. Rev.* **2000**, *100*, 1479. (b) Gibson, V. C.; Spitzmesser, S. K. *Chem. Rev.* **2003**, *103*, 283.

(2) (a) Mecking, S. *Coord. Chem. Rev.* **2002**, *203*, 325. (b) Zuideveld, M. A.; Wehrmann, P.; Röhr, C.; Mecking, S. *Angew, Chem., Int. Ed.* **2004**, *43*, 869.

(3) Hagman, J. F.; Crary, J. W. *Encyclopedia of Polymer Science and Engineering*; Mark, H. F., Bikales, N. W., Overberger, C. G., Menges, G., Kroschwitz, J. I., Eds.; Wiley: New York, 1985; Vol. 1, p 325.

(4) Stockland, R. A., Jr.; Foley, S. R.; Jordan, R. F. *J. Am. Chem. Soc.* **2003**, *125*, 796.

(5) (a) Ittel, S. D.; Johnson, L. K.; Brookhart, M. *Chem. Rev.* **2000**, *100*, 1169. (b) Johnson, L. K.; Killian, C. M.; Brookhart, M. *J. Am. Chem. Soc.* **1995**, *117*, 6414. (c) Killian, C. M.; Tempel, D. J.; Johnson, L. K.; Brookhart, M. *J. Am. Chem. Soc.* **1996**, *118*, 11664. (d) Mecking, S.; Johnson, L. K.; Wang, L.; Brookhart, M. *J. Am. Chem. Soc.* **1998**, *120*, 888. (e) Johnson, L. K.; Mecking, S.; Brookhart, M. *J. Am. Chem. Soc.* **1996**, *118*, 267. For other late-transition-metal ethylene polymerization catalysts, see the following reviews: (f) Britovsek, G. J. P.; Gibson, V. C.; Wass, D. F. *Angew, Chem., Int. Ed.* **1999**, *38*, 428. (g) Britovsek, G. J. P.; Gibson, V. C.; Hoarau, O. D.; Spitzmesser, S. K.; White, A. J. P.; Williams, D. J. *Inorg. Chem.* **2003**, *42*, 3454. (h) Foley, S. R.; Stockland, R. A., Jr.; Shen, H.; Jordan, R. F. *J. Am. Chem. Soc.* **2003**, *125*, 4350. (i) Helldörfer, M.; Backhaus, J.; Milius, W.; Alt, H. G. *J. Mol. Catal. A* **2003**, *193*, 59.

(6) (a) Younkin, T. R.; Connor, E. F.; Henderson, J. I.; Friedricj, S. K.; Grubbs, R. H.; Bansleben, D. A. *Science* **2000**, *287*, 460. (b) Wang, C.; Friedrich, S.; Younkin, T. R.; Li, R. T.; Grubbs, R. H.; Bansleben, D. A.; Day, M. W. *Organometallics* **1998**, *17*, 3149.

(7) (a) Keim, W.; Kowalt, F. H.; Goddard, R.; Krüger, C. *Angew, Chem., Int. Ed.* **1978**, *17*, 466. (b) Drent, E.; Van Dijk, R.; Van Ginkel, R.; Van Oort, Z. B.; Pugh, R. I. *Chem. Commun.* **2002**, 744. (c) Drent, E.; Van Dijk, R.; Van Ginkel, R.; Van Oort, Z. B.; Pugh, R. I. *Chem. Commun.* **2002**, 964.

(8) (a) Komon, Z. J. A.; Bu, X.; Bazan, G. C. *J. Am. Chem. Soc.* **2000**, *122*, 1830. (b) Komon, Z. J. A.; Bu, X.; Bazan, G. C. *J. Am. Chem. Soc.* **2000**, *122*, 12379. (c) Lee, B. Y.; Bu, X.; Bazan, G. C. *Organometallics* **2001**, *20*, 5425. (d) Kim, Y. H.; Kim, T. H.; Lee, B. Y.; Woodmansee, D.; Bu, X.; Bazan, G. C. *Organometallics* **2002**, *21*, 3082. (e) Komon, Z. J. A.; Diamond, G. M.; Leclerc, M. K.; Murphy, V.; Okazaki, M.; Bazan, G. C. *J. Am. Chem. Soc.* **2002**, *124*, 15280. (f) Shim, C. B.; Kim, Y. H.; Lee, B. Y.; Dong, Y.; Yun, H. *Organometallics* **2003**, *22*, 4272.

(9) (a) Thomas, J. C.; Peters, J. C. *Inorg. Chem.* **2003**, *42*, 5055. (b) Lu, C. C.; Peters, J. C. *J. Am. Chem. Soc.* **2002**, *124*(19), 5272.

(10) Philipp, D. M.; Muller, R. P.; Goddard, W. A.. III; Storer, J.; McAdon, M.; Mullins, M. *J. Am. Chem. Soc.* **2002**, *124*, 10198.

(11) von Schenck, H.; Stromberg, S.; Zetterberg, K.; Ludwig, M.; Akermark, B.; Svensson, M. *Organometallics* **2001**, *20*, 2813.

10.1021/om049018z CCC: $30.25
Publication on Web 03/31/2005

Scheme 1. π vs σ Complex Formation

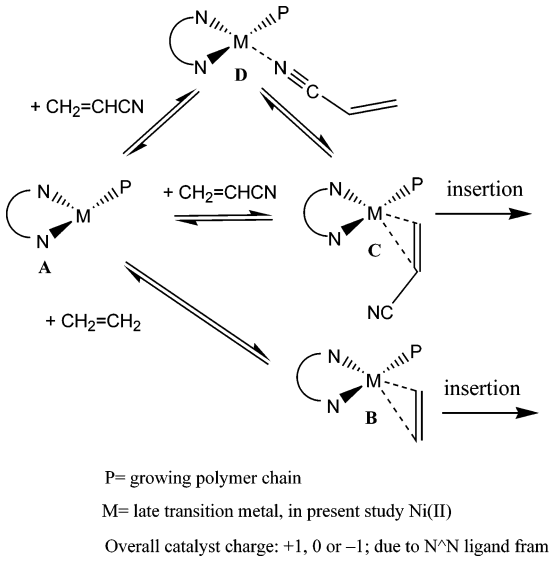

preferably be energetically more feasible than the σ bonding of CN to the metal, or poisoning will occur. A theoretical study by Deubel and Ziegler[12a] has shown that cationic Brookhart catalysts based on both Pd(II) and Ni(II) metal centers prefer σ bonding to AN, although the preference is most pronounced for Ni(II). In moving to the neutral Grubbs type catalysts, σ bonding is still preferred for Ni(II) but the margin is much smaller and for Pd(II) the preference shifts from σ to π coordination. It would thus appear that neutral catalysts are more promising than cationic systems and Pd(II) more appropriate than Ni(II). In fact, one might expect anionic catalysts to be even better in terms of less poisoning, since the negative AN nitrogen would be repelled by an anionic metal fragment, whereas the π complexation should be enhanced by increased metal to ligand back-donation. By itself, the cationic Ni(II) diimine Brookhart catalyst is poisoned substantially.[12c,e] To improve on this unfavorable situation, the original Brookhart catalyst will be modified to make it neutral or even anionic. For each modification the preference (poisoning) for AN σ coordination over π bonding will be calculated. In a subsequent study[13] the systems with the least poisoning will be selected for further tests of polymerization activity by calculating their barrier of insertion (Scheme 2).

The first series of modifications involve the backbone of the diimine ring (Chart 1), where we replace the alkyl group R_1 by a number of anionic substituents (BH_3^-, BF_3^-, etc.) or a ring carbon by B^-. In all cases we monitor primarily the influence of a negative substituent on the metal center.

Charts 2 and 3 consider substitutions on the aryl ring in the ortho, meta, and para positions. Here we probe

Scheme 2. Insertion of Ethylene and Acrylonitrile into the Ni–Alkyl Bond

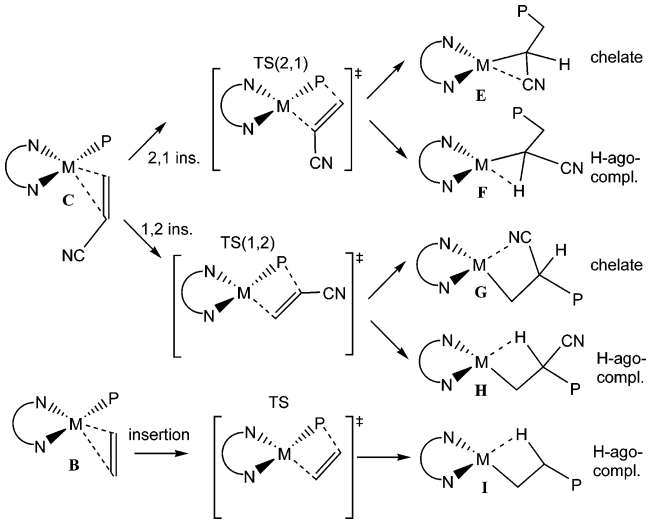

Chart 1. Backbone-Substituted Neutral Ni–Diimine Complexes

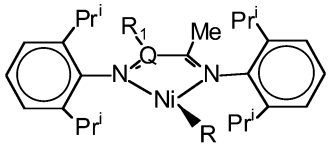

R=Me, Pr^n or CH(CN)Et

ID	R_1	Q
0	Me	=C-
1	BH_3^-	
2	BF_3^-	
3	BMe_3^-	
4	SO_3^-	
5	OBH_3^-	
6	$OAlH_3^-$	
7	OBF_3^-	
8	$OAlF_3^-$	
9	$OBMe_3^-$	
10	H	=B-

Chart 2. Side-Group-Substituted Neutral Ni–Diimine Complexes

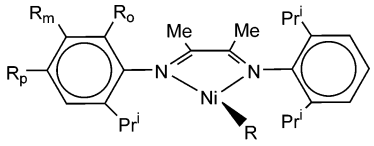

ID	R_p	R_m	R_o
11	BH_3^-	H	^{i}Pr
12	H	BH_3^-	^{i}Pr
13	H	H	$BHMe_2^-$

the distance of the negative substituent from the Ni(II) center and, in the case of the ortho position, a direct bond between Ni(II) and the anionic group. Finally, Chart 4 introduces an alkyl chain connecting the aryl rings. The chain allows for the positioning of anionic groups at different distances from the Ni(II) center.

Unfortunately, little or no poisoning is only one requirement for a good polar copolymerization catalyst. Another is a low barrier for the insertion of AN into the metal–carbon bond after the π complex is formed. Here

(12) (a) Deubel, D. V.; Ziegler, T. *Organometallics* **2002**, *21*, 1603. (b) Deubel, D. V.; Ziegler, T. *Organometallics* **2002**, *21*, 4432. (c) Michalak, A.; Ziegler, T. *Organometallics* **2001**, *20*, 1521. (d) Michalak, A.; Ziegler, T. *J. Am. Chem. Soc.* **2001**, *123*, 12266. (e) Michalak, A.; Ziegler, T. *Organometallics* **1999**, *18*, 3998. (f) Michalak, A.; Ziegler, T. *Organometallics* **2000**, *19*, 1850. (g) Michalak, A.; Ziegler, T. *Organometallics* **2003**, *22*, 2660. (h) Szabo, M. J.; Jordan, R. F.; Michalak, A.; Piers, W. E.; Weiss, T.; Yang, S.-Y.; Ziegler, T. *Organometallics* **2004**, *23*, 5565.

(13) Szabo, M. J.; Galea, N. M.; Mickalak, A.; Yang, S.-Y.; Groux, L. F.; Piers, W. E.; Ziegler, T. Manuscript in preparation.

Chart 3. Neutral and Anionic Ni−Diimine Complexes with Ortho Phenyl Anionic Groups and Various Bulky Substituents at the Backbone

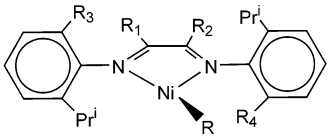

R=Me, Pr^n or CH(CN)Et

ID	R_1	R_2	R_3	R_4
14	Me	Me	^iPr	^iPr
15	Me	Me	CF_3	^iPr
16	Me	Me	BF_3^-	^iPr
17	Me	Me	SO_3^-	^iPr
18	Me	Me	OBF_3^-	^iPr
19	CF_3	CF_3	BF_3^-	^iPr
20	^tBu	^tBu	BF_3^-	^iPr
21	^tBu	^tBu	SO_3^-	^iPr
22	Me	Me	BF_3^-	BF_3^-
23	CF_3	CF_3	BF_3^-	BF_3^-
24	^tBu	^tBu	BF_3^-	BF_3^-

Chart 4. Neutral Ni-Diimine Complexes with an Alkyl Bridge between the Two Side Groups

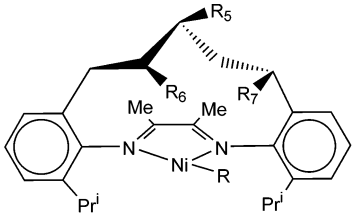

ID	R_5	R_6	R_7
25	BF_3^-	H	H
26	$CH_2BF_3^-$	H	H
27	$(CH_2)_2BF_3^-$	H	H
28	H	BF_3^-	H
29	H	H	BF_3^-

both experimental[5g,h] and theoretical studies[12] have shown that Ni(II) complexes have a lower barrier than their Pd(II) homologues. Further calculations[12h] demonstrate that the barrier of insertion increases with the electron density on the metal from cationic to anionic complexes. Because opposing factors optimize the barriers of insertion and the lack of poisoning, a compromise has to be struck in designing a good polar copolymerization catalyst. This aspect will be covered in a special discussion on the kinetics of homopolymerization and polar copolymerization.

The use of negative substituents to reduce poisoning has already been attempted experimentally by Bazan,[8b] Peters,[9] and Piers.[14] It has further been suggested on the basis of theoretical calculations by Michalak,[12c−g] Deubel,[12a,b] and Szabo.[12h] However, this is the first time where this idea has been pursued systematically.

Computational Details

Molecular geometries have been optimized at the level of gradient-corrected density functional theory using the Becke−Perdew exchange-correlation functional.[15−17] The calculations have been carried out with the Amsterdam Density Functional (ADF 2004) program package developed by Baerends et al.[18,19] and vectorized by Ravenek.[20,21] The numerical integration scheme applied to the calculations was developed by te Velde et al.[22] The geometry optimization procedure was based on the method of Versluis and Ziegler.[23] For nickel ($n = 3$) a standard triple-ζ STO basis set, from the ADF database IV, was employed with ns, np, nd, $(n + 1)$s, and $(n + 1)$p treated as valence and the rest as frozen core. For the nonmetal elements a standard double-ζ basis set with one set of polarization functions (ADF database III) was applied, with frozen cores including 1s electrons for B, C, N, and O and 1s2s2p for Al.[24,25] Auxiliary[26] s, p, d, f, and g STO functions centered on all nuclei were used to fit the Coulomb and exchange potentials during the SCF process. The reported relative energies include scalar relativistic corrections.[27−29] All structures shown correspond to minimum points on the potential surface. No symmetry constraints were used.

The combined DFT and molecular mechanics calculations were performed using the quantum mechanics/molecular mechanics (QM/MM) implementation in the ADF program.[30] An augmented Sybyl molecular mechanics force field[31] was utilized to describe the molecular mechanics potential, which includes van der Waals parameters from the UFF force fields[32] for nickel and boron.

Calculations have been carried out studying the solvent effect using the COSMO model. On the basis of the results we expect only minor effects due to the solvent (toluene) on the actual bonding energies of ethylene and acrylonitrile.

For both backbone and side-group-substituted zwitterionic candidates a specific partitioning format was applied, as illustrated in Chart 5. The quantum mechanical part contains the generic metal−diimine complex including an anionic group at the catalyst backbone (**1**−**10**) or an anionic substituted phenyl group (**11**−**13**). The rest of the molecule, including the aryl group(s) and Me group(s) on the backbone, are treated in the molecular mechanics region. Ratios, α, of 1.40 and 1.34 were employed for the N(sp^2)−C(aryl) and C(sp^2)−C(sp^3) link bonds, respectively, to reproduce the average experimental bond distances[8] for related compounds. For the cationic Ni complex (**0**), a link bond ratio α of 1.385 for the N−C(aryl) and a link bond ratio of 1.380 for the backbone C(sp^2)−Me bond was adopted from Woo et al.[33]

(14) Groux, L. F.; Weiss, T.; Reddy, D. N.; Chase, P. A.; Piers, W. A.; Ziegler, T.; Parvez, M.; Benet-Buchholz, J. *J. Am. Chem. Soc.* **2005**, *127*, 1854.
(15) Becke, A. *Phys. Rev. A* **1988**, 38, 3098.
(16) Perdew, J. P. *Phys. Rev. B* **1986**, 34, 7406.
(17) Perdew, J. P. *Phys. Rev. B* **1986**, 33, 8822.
(18) Baerends, E. J. Ph.D. Thesis, Free University, Amsterdam, The Netherlands, 1973.
(19) Baerends, E. J.; Ellis, D. E.; Ros, P. *Chem. Phys.* **1973**, 2, 41.
(20) Ravenek, W. In *Algorithms and Applications on Vector and Parallel Computers*; te Riele, H. J. J., Dekker: T. J., van de Horst, H. A., Eds.; Elsevier: Amsterdam, The Netherlands, 1987.
(21) Boerrigter, P. M.; te Velde, G.; Baerends, E. J. *Int. J. Quantum Chem.* **1988**, 33, 87.
(22) te Velde, G.; Baerends, E. J. *J. Comput. Chem.* **1992**, 99, 84.
(23) Versluis, L.; Ziegler, T. *J. Chem. Phys.* **1988**, 88, 322.
(24) Snijders, J. G.; Baerends, E. J.; Vernoijs, P. *At. Nucl. Data Tables* **1982**, 26, 483.
(25) Vernoijs, P.; Snijders, J. G.; Baerends, E. J. Slater Type Basis Functions for the Whole Periodic System; Internal report (in Dutch); Department of Theoretical Chemistry, Free University, Amsterdam, The Netherlands, 1981.
(26) Krijn, J.; Baerends, E. J. Fit Functions in the HFS Method; Internal Report (in Dutch); Department of Theoretical Chemistry, Free University, Amsterdam, The Netherlands, 1984.
(27) Ziegler, T.; Tschinke, V.; Baerends, E. J.; Snijders, J. G.; Ravenek, W. *J. Phys. Chem.* **1989**, *93*, 3050.
(28) Snijders, J. G.; Baerends, E. J. *Mol. Phys.* **1978**, *36*, 1789.
(29) Snijders, J. G.; Baerends, E. J.; Ros, P. *Mol. Phys.* **1979**, *38*, 1909.
(30) Woo, T. K.; Cavallo, L.; Ziegler, T. *Theor. Chem. Acc.* **1998**, *100*, 307.
(31) Clark, M.; Cramer, R. D., III; van Opdenbosch, N. *J. Comput. Chem.* **1989**, *10*, 982.
(32) Rappe, A. K.; Casewit, C. J.; Colwell, K. S.; Goddard, W. A., III; Skiff, W. M. *J. Am. Chem. Soc.* **1992**, *114*, 10024.

Chart 5 Partitioning of the System into Molecular Mechanics (in Dotted Area) and Quantum Mechanics Regions

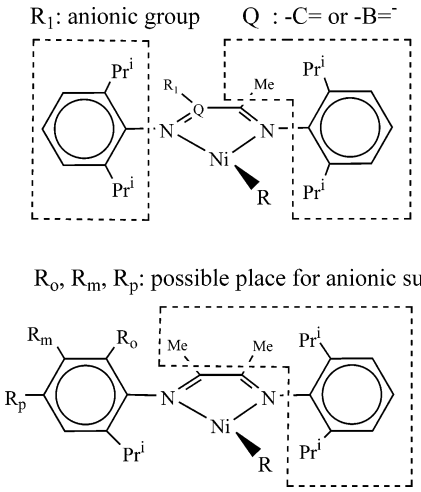

Kinetic Aspects of Ethylene Homopolymerization and Ethylene/Acrylonitrile Copolymerization

In ethylene/acrylonitrile copolymerization we have chain propagation by insertion of both ethylene and acrylonitrile into the polymer. We shall now discuss the kinetics of both processes starting with ethylene propagation. The generally accepted mechanism for chain propagation by ethylene in coordination polymerization[1] is shown in Scheme 3A. These reactions, from a kinetic point of view, are analogous to Michaelis−Menten type processes.[34] In the first step, ethylene can reversibly bind to the catalytically active species to yield the intermediate olefin π complex. Once bound, the monomer can insert into the metal−alkyl bond. The major difference from the Michaelis−Menten reactions is that the insertion product is itself an active species, which can uptake an other olefin to continue the catalytic cycle. Thus, for the reaction depicted in Scheme 3A, using the mass balance $[A'] = A_0 - [C']$, where A_0 is the initial catalyst concentration, the initial rate of the polymerization can be obtained as shown in eq 1, where B'_0 is the initial monomer concentration.

$$k_{ET} = \frac{k_2 k_1 A_0 B'_0}{k_1 B'_0 + k_1^{-1} + k_2} \qquad (1)$$

The efficiency of any late-transition-metal polymerization catalyst candidates, which work in the same manner as shown in Scheme 3, can be characterized by using eq 1.

Figure 1 displays $\log(k_{rel})$, the log of the relative rate

$$k_{rel} = k_{ET}{}^0/k_{ET} \qquad (2)$$

where $k_{ET}{}^0$ is the rate of ethylene propagation for the original cationic Brookhart catalyst (BR) according to eq 1 and k_{ET} is the rate of ethylene propagation for a general catalyst with rate constants k_1, $k_1{}^{-1}$ and k_2, again according to eq 1. Thus, $\log(k_{rel}) > 0$ means that the general catalyst has a lower rate of propagation than BR. The graph in Figure 1 displays $\log(k_{rel})$ values for different values of internal insertion barrier $\Delta E^{\ddagger}$ that

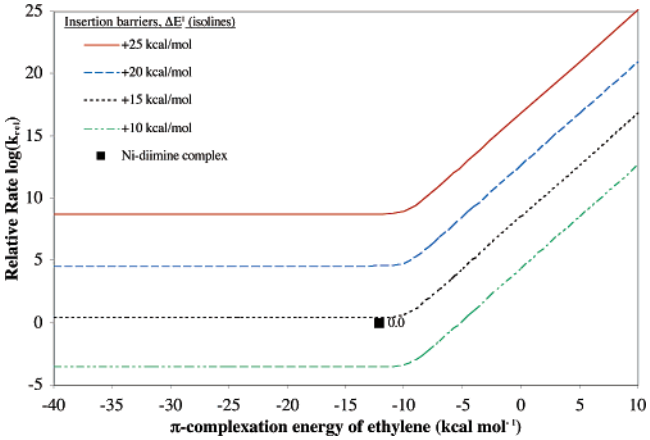

Figure 1. Log of the relative rate ($k_{rel} = k_{ET}{}^0/k_{ET}$) for ethylene propagation as a function of the ethylene complexation energy (ΔE_π) for different internal insertion barriers ($\Delta E^{\ddagger}$). k_{ET} is the rate of ethylene propagation for a general catalyst and $k_{ET}{}^0$ is the rate of ethylene propagation for the original cationic Brookhart catalyst according to eq 1.

Scheme 3 Mechanism of Chain Propagation for Late-Transition-Metal Polymerization

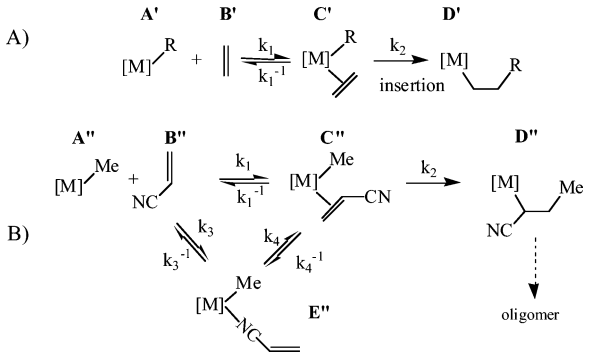

are related to k_2 and different values of π complexation energy that are related to $k_1{}^{-1}$. Thus, a low $\Delta E^{\ddagger}$ leads to a high rate constant k_2 and a strong complexation affords a low rate constant $k_1{}^{-1}$ for complex dissociation. Finally, molecular dynamic simulations[35] on BR have shown that k_1 is related to a barrier of ~9 kcal mol^{-1} due to the entropic loss when the monomer is captured. The rate constant k_1 is going to be nearly the same for different catalyst and monomers. It should be mentioned that $k_{ET}{}^0$ is calculated for the insertion of ethylene into the Ni−propyl bond of the cationic Brookhart diimine catalyst, with $\Delta E_\pi = -12.2$ kcal mol^{-1} and $\Delta E^{\ddagger} = 14.5$ kcal mol^{-1}.

The reaction rate constants k_1, $k_1{}^{-1}$, and k_2 have been calculated by the standard Eyring equation. This model, however, contains several assumptions. We calculated the ratio of the reaction rates at $T = 263$ K and $p = 1$ bar. Under these conditions the ethylene concentration in toluene[36] is 0.23 mol dm^{-3}. Since the catalyst concentration is much lower than the ethylene concentration, we also assume that the olefin concentration B' is constant: B'_0.

(33) Woo, T. K.; Ziegler, T. *J. Organomet. Chem.* **1999**, *591*, 204.
(34) Peuckert, M.; Keim, W. *Organometallics* **1983**, *2*, 594.
(35) Woo, T. K.; Blöchl, P. E.; Ziegler, T. *J. Phys. Chem. A* **2000,** *104*, 121.
(36) Waters, J. A.; Mortimer, G. A.; Clements, H. E. *J. Chem. Eng. Data* **1970**, *15*, 174.

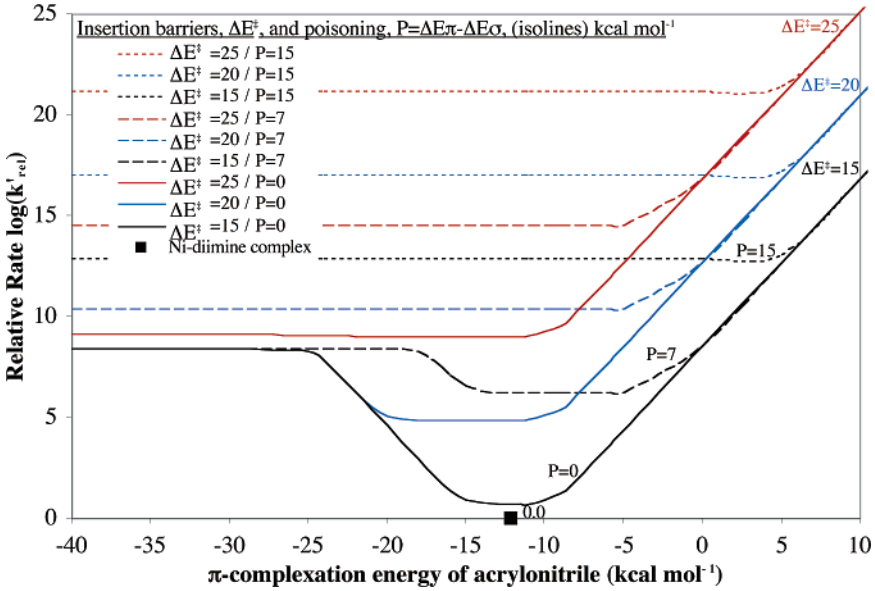

Figure 2. The log of the relative rate ($k'_{rel} = k_{ET}{}^0/k_{AN}$) for acrylonitrile propagation as a function of the acrylonitrile π complexation energies (ΔE_π) for different internal insertion barriers ($\Delta E^\ddagger$) and poisoning P. k_{AN} is the rate of acrylonitrile propagation for a general catalyst according to eq 3 and $k_{ET}{}^0$ is the rate of ethylene propagation for the original cationic Brookhart catalyst according to eq 1.

For the type of late-metal catalyst under consideration here, the internal barrier of insertion[12] $\Delta E^\ddagger$ is 15 kcal mol^{-1} or above and, thus, is higher than the uptake barrier[37] ($\sim$ 9 kcal mol^{-1}). We can as a consequence assume that $k_1 > k_2$. There are now two limiting cases to consider for k_{ET} in relation to k_{rel} and Figure 1. The first is a strong π complexation (left side of Figure 1) where $\Delta E_\pi < -35$ kcal mol^{-1}. In that case $k_1{}^{-1} < k_1$, k_2 and $k_{ET} \approx k_2A_0$. Thus, the rate of propagation as well as 1/log(k_{rel}) decreases exponentially with the internal insertion barrier but is independent of k_1 and $k_1{}^{-1}$. The second limiting case is weak π complexation with $\Delta E_\pi > 0$ (right side of Figure 1). In this case $k_1{}^{-1} > k_1$, k_2 and $k_{ET} \approx (k_1/k_1{}^{-1})k_2A_0B'_0$. Now the propagation rate depends on k_2 as well as the equilibrium constant ($k_1/k_1{}^{-1}$). Thus, the propagation rate and 1/log(k_{rel}) will decrease as the π complexation becomes weaker. It is clear from the considerations given here that a good ethylene polymerization catalyst should have a low barrier of insertion and a strong π complexation ($\Delta E_\pi \leq -10$ kcal mol^{-1}).

Turning next to chain propagation by acrylonitrile uptake and insertion, we note that the kinetics is more complex than for pure ethylene, as illustrated in Scheme 3B. Thus, acrylonitrile can, in addition to π complexation (k_1, $k_1{}^{-1}$) and insertion (k_2), also coordinate through $-$CN σ complexation (k_3, $k_3{}^{-1}$). Finally the σ complex can interconvert to the π complex (k_4) without ligand dissociation and vice versa ($k_4{}^{-1}$). The rate of propagation for acrylonitrile according to Scheme 3B is given by

$$k_{AN} = \frac{k_2\left[(k_1A_0B_0'') - \dfrac{k_3B_0''A_0(k_1B_0'' - k_4)}{k_3B_0'' + k_3{}^{-1} + k_4}\right]}{k_1B_0'' + k_1{}^{-1} + k_2 + k_4{}^{-1} - \dfrac{(k_3B_0'' - k_4{}^{-1})(k_1B_0'' - k_4)}{k_3B_0'' + k_3{}^{-1} + k_4}} \quad (3)$$

under the assumption of constant acrylonitrile concentration B_0''. We have found the barrier for interconversion between the σ complex E$''$ and the π complex C$''$ to be $\Delta E_4{}^\ddagger = 25$ kcal mol^{-1} ($\Delta E_4{}^{-1\ddagger} = \Delta E_4{}^\ddagger - \Delta E_\pi + \Delta E_\sigma$) for the cationic diimine Brookhart catalyst, and we shall use this value as an estimate for all systems.

The uptake rate constants k_1 and k_3 are again determined from the entropic uptake barriers of 9 kcal mol^{-1}, whereas $k_1{}^{-1}$ and $k_3{}^{-1}$ are determined from the uptake barrier as well as the π complexation energy ΔE_π and σ complexation energy ΔE_σ, respectively. We shall in the following refer to $\Delta E_\pi - \Delta E_\sigma$ as the poisoning P. Figure 2 displays the log of the ratio

$$k'_{rel} = k_{ET}{}^0/k_{AN} \quad (4)$$

as a function of ΔE_π for different values of P and $\Delta E^\ddagger$. Here $k_{ET}{}^0$ is again the same propagation rate for ethylene whereas k_{AN} is the propagation rate for acrylonitrile according to eq 3.

There are three limiting cases for k_{AN} in relation to k'_{rel} and Figure 2. The first two are for a strong π complexation (left side of Figure 2), where $k_3{}^{-1}$, $k_1{}^{-1} \ll k_1$, k_2, k_3. If $k_2 < k_4{}^{-1}$, $k_{AN} \approx k_2(k_4/k_4{}^{-1})A_0$ and in this case the rate of propagation of acrylonitrile and 1/log(k'_{rel}) decrease with the insertion barrier and the poisoning P through the equilibrium constant ($k_4/k_4{}^{-1}$). Note that for $P = 0$ the limit is the same as for pure ethylene, since $k_4/k_4{}^{-1}$ in that case is 1. If $k_2 > k_4{}^{-1}$, $k_{AN} \approx k_4A_0$ and the rate of propagation of acrylonitrile and log(k'_{rel}) depends only on the barrier for interconversion between the σ and π complexes. The third limiting case is weak π complexation with $\Delta E_\pi > +10$ (right side of Figure 2). In this case $k_1{}^{-1}$ and $k_3{}^{-1}$ are the dominating rate constants and $k_{AN} \approx (k_1/k_1{}^{-1})k_2A_0B_0''$. Thus, this limit becomes the same as for ethylene and is independent of P. We note again that at this limit the propagation

(37) Deng, L.; Ziegler, T.; Woo, T. K.; Margl, P.; Fan, L. *Organometallics* **1998,** *17*, 3240.

Table 1. Relative Energies (kcal mol^{-1}) of the Acrylonitrile and Ethylene π and σ Complexes with Various Anionic Substitutions at the Backbone of the Ni−Diimine Type Catalyst

ID	anionic group	R	ET	AN		
			π	π	σ	$\pi-\sigma$
0		Me	−34.2	−27.5	−49.5	22.0
1	BH_3^-	Me	−29.3	−30.2	−38.6	8.4
2	BF_3^-	Me	−29.4	−28.0	−39.2	11.2
3	BMe_3^-	Me	−26.9	−27.6	−37.2	9.6
4	SO_3^-	Me	−31.1	−29.9	−40.9	11.0
5	OBH_3^-	Me	−33.8	−34.3	−41.4	7.1
6	$OAlH_3^-$	Me	−34.2	−34.4	−42.3	7.9
7	OBF_3^-	Me	−33.7	−32.2	−40.8	8.6
8	$OAlF_3^-$	Me	−34.0	−31.7	−41.0	9.3
9	$OBMe_3^-$	Me	−31.0	−31.7	−41.2	9.5
10	$-B^-$	Me	−28.4	−31.3	−37.9	6.6

rate and $1/\log(k'_{rel})$ will decrease as the π complexation becomes weaker.

Inspection of Figure 2 reveals that the best propagation rates for a given $\Delta E^{\ddagger}$ and poisoning are obtained when $k_2 > k_4^{-1}$ for π complexations in the region $\Delta E_\pi > -20$ and $\Delta E_\pi < -5$ kcal mol^{-1}; as an example, see the isoline for $\Delta E^{\ddagger} = 15$ kcal mol^{-1} and $P = 0$ kcal mol^{-1}. Thus, in this region increasing the barrier of insertion from $\Delta E^{\ddagger} = 15$ kcal mol^{-1} to $\Delta E^{\ddagger} = 24$ kcal mol^{-1} will only decrease $\log(k'_{rel})$ by a factor of 8 for $P = 0$. We will keep this in mind as we now turn to study π complexation and poisoning in complexes between acrylonitrile and Brookhart type diimine complexes that have been modified by anionic substitution.

Results and Discussion

Enhancing π Complexation Compared to N Coordination. The original cationic nickel Brookhart catalyst has, as already mentioned,[12a] a preference of 22.0 kcal mol^{-1} with an R = Me polymer chain (**0**) for σ coordination to acrylonitrile. We shall in the following examine to what degree this preference can be reduced by introducing neutral zwitterionic Brookhart type Ni complexes with various anionic backbone and side-group substituents (Charts 1−3).

Backbone Substitution of the Ni−Diimine Type Brookhart Catalyst. We shall begin our investigation by exploring the effect of replacing a methyl group on the diimine backbone (Chart 1) by anionic substituents. Table 1 presents π complexation energies for ethylene and acrylonitrile as well as σ bonding energies for acrylonitrile, all based on QM/MM calculations. The corresponding complexation energies for the cationic Brookhart complex (**0**) are also given in Table 1, as a reference.

It follows from a comparison between compound **0** and the zwitterionic systems (**1**−**10**) that the preference for σ-complexation indeed is reduced (by 11−16 kcal mol^{-1}) after the anionic substitution. This has been primarily accomplished by the anticipated reduction in the acrylonitrile σ bond energy. It is also clear from Table 1 that the individual anionic groups (Y^-) used in substitution give rise to certain variations in the ethylene and acrylonitrile complexation energies as well as the preference for σ coordination. These variations cannot be understood without taking into account the steric influence of the substituent Y^-. The anionic substituent makes the two sites occupied by the methyl group and the monomer (L), acrylonitrile or ethylene, inequivalent, with methyl preferring to be trans to Y^- (Chart 6). The Y^- group will to some degree further interact sterically with the aryl ring, resulting in a change in the $C_1'-N-C_3'$ angle. This change will in turn influence the steric interaction between the aryl group and L. Thus, Y^- can sterically change the complexation energy of L. This factor is clearly seen for $Y = BH_3^-$, BF_3^-, and BMe_3^-, where the order of the binding energies in each of the two π complexation modes follows the trend $BH_3^- > BF_3^- > BMe_3^-$ in absolute terms.

Chart 6. Geometric Parameters for the Backbone-Substituted Complexes

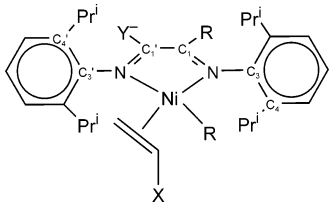

Table 2. Relative Energies (kcal mol^{-1}) of the Acrylonitrile and Ethylene π and σ Complexes with Various Anionic Substitutions on the Aryl Group of the Ni−Diimine Type Complex

ID	anionic group	R	ET	AN		
			π	π	σ	$\pi-\sigma$
11	*p*-BH_3^-	Me	−20.2	−18.8	−34.2	15.4
12	*m*-BH_3^-	Me	−21.5	−19.9	−34.5	14.6
13	*o*-$BHMe_2^-$	Me	−11.3	−14.2	−13.2	−1.0

In going from BX_3^- to OBX_3^- and $OAlX_3^-$, one would expect a reduction in the steric interaction with the aryl group resulting in an increase in the strength of the π complexation energies ($BX_3^- < OBX_3^- < OAlX_3^-$), in agreement with the calculated numbers. Further, among BX_3^- substituents, BF_3^- gives rise to the strongest σ bond, as a result of its electron-withdrawing ability, which enhances the M−NC bond strength. Complex **10**, with a carbon in the chain substituted by a B^- unit, is sterically closest to Brookhart's original catalyst. Thus, its reduction of the preference for σ complexation to only 6.6 kcal mol^{-1} is largely electronic. Complexes **1**−**10** are not promising candidates in terms of π complexation and poisoning, according to the discussion given in the previous section on kinetics.

Anionic Substitution on the Aryl Group of the Ni−Diimine Type Complex. We shall next move from the diimine backbone to the aryl side group and substitute a para or meta hydrogen by BH_3^-. The ortho position holding the *i*-Pr group will also be substituted. However, the replacement will be $BHMe_2^-$, rather than BH_3^-, to maintain some of the steric bulk exerted by the *i*-Pr group. The calculated complexation energies are given in Table 2, and the complexes (**11**−**13**) are shown in Chart 2. Only the energies of the most stable isomers are shown.

The QM/MM calculations underline that anionic substitutions in the para and meta positions only have a marginal influence on the preference for σ complexation with 15.4 kcal mol^{-1} for para (**11**) and 14.6 kcal mol^{-1} for meta (**12**) compared to 22.0 kcal mol^{-1} for the original Brookhart catalyst (**0**). In contrast, the π and σ complexes of **13** are destabilized by about 6 and 21 kcal mol^{-1}, respectively, compared to the meta (**12**)- and

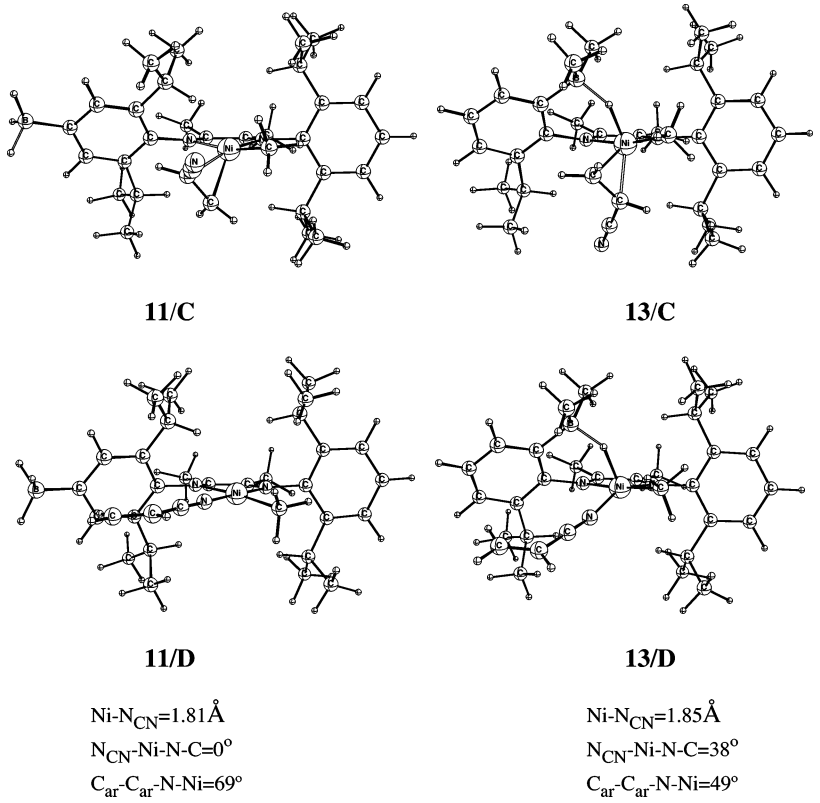

Figure 3. Optimized QM/MM molecular structure of *p*-BH_3^- and *o*-$BHMe_2^-$ substituted complexes.

para-substituted (**11**) complexes. The σ complex is destabilized 15 kcal mol^{-1} more than the π complexes; thus, the $\Delta E_\pi - \Delta E_\sigma$ poisoning value is reduced to -1 kcal mol^{-1}. In fact, the π complexation mode becomes favored over the σ binding. This functional group tolerance in **13** is the best we have encountered so far.

One may rationalize the difference among **11**, **12**, and **13** by comparing the molecular structure of the extraordinarily tolerant ortho complex **13** and the highly poisoned para and meta complexes **11** and **12**. The molecular structures of the σ-acrylonitrile complexes are shown in Figure 3. In the ortho zwitterionic complex **13** the anionic $BH(Me)_2^-$ group is much closer to the Ni center than in structures **11** and **12**. The ortho anionic group is able to establish a direct contact to the Ni center, with a 1.6 Å Ni−H distance, while the para-substituted complex can only influence the metal center via the 2,6-C_6H_3(*i*-Pr)$_2$ phenyl ring. There is a clear competition between the CN group and the ortho anionic substituent. This can be seen by comparing the σ complex structures of **11** and **13**. The Ni−N bond distance is longer in complex **13** than in complex **11** by 0.04 Å, indicating the destabilization of the N-binding mode in the ortho-substituted complex **13**. Looking at the N−Ni−N−C dihedral angles, one can see that the acrylonitrile is forced out from the diimine plane by 38° (Figure 3). The ortho-substituted aryl ring is also rotated by 20°, driven by the direct $BHMe_2^-$−Ni interaction. The C−C−N−Ni dihedral angles are 49° and 69° in complexes **11** and **13**, respectively. The ortho anionic group destabilizes the π complex as well, but the destabilization is larger for the σ complex than for the π complex.

Further Anionic Ortho Substitution in the Aryl Group of the Ni−Diimine Type Complex. The ortho substitution motif shows great promise in terms of reducing the poisoning, and we shall in the following consider different anionic substituents (see **15**−**21** in Chart 3). Further, we shall consider not only *n*-propyl but also Me and CH(CN)Et as the growing chain R. The complexation energies of the ethylene and acrylonitrile π and σ complexes are shown in Table 3.

We shall start our discussion with the neutral zwitterionic complex **16**, in which the ortho hydrogen atom of one of the aryl rings is substituted with a BF_3^- group. The poisoning is ∼1 kcal mol^{-1} with both Me and *n*-Pr as the growing chain. A growing chain with an α-CN group has a poisoning by 5.8 kcal mol^{-1}, since the strongly electron withdrawing CN group makes the metal center more electrophilic.

The SO_3^- group containing complex **17** is more tolerant to the polar CN group than is complex **16**, with a BF_3^- substituent. Both σ and π complexes are destabilized in comparison to BF_3^- derivatives, but σ complexes are destabilized more, thus reducing the poisoning by 4.7, 4.0, and 4.4 kcal mol^{-1} for R = Me, *n*-propyl, CH(CN)Et chain, respectively.

Complex **16** and **17** exhibit exceptional tolerance toward the polar CN group. To understand better the role of the BF_3^- and SO_3^- groups, we looked at the bond orders of the alkyl complexes **16A** and **17A** and the corresponding π and N complexes **16B**−**D** and **17B**−**D** (see Chart 7), using the ADF implementation of the Nalewajski−Mrozek[38] bond-order scheme. Both BF_3^- and SO_3^- groups exhibit a direct contact to the metal center with R(Ni−F) = 1.90 Å and R(Ni−O) = 1.89 Å for complexes **16A** and **17A**, respectively. The corresponding bond orders for the alkyl complexes (**A**) are 0.32 and 0.47 for the Ni−F and Ni−O bonds. It is further worth mentioning that the B−F and S−O

Table 3. Relative Energies (kcal mol^{-1}) of the Acrylonitrile and Ethylene π and σ Complexes with Various Anionic Ortho Substitutions on the Aryl Ring of the Ni−Diimine Type Complex

ID	R_3	R_4	R_1, R_2	R	ET π	AN π	AN σ	AN $\pi-\sigma$
15	CF_3	^{i}Pr	Me	Me	−25.8	−21.9	−39.3	17.4
16	BF_3^-	^{i}Pr	Me	Me	−13.8	−15.8	−17.1	1.3
				^{n}Pr	−12.5	−16.3	−17.4	1.1
				CH(CN)Et	−14.4	−17.0	−22.8	5.8
17	SO_3^-	^{i}Pr	Me	Me	−10.9	−15.0	−11.6	−3.4
				^{n}Pr	−10.0	−15.4	−12.5	−2.9
				CH(CN)Et	−13.3	−17.2	−18.6	1.4
18	OBF_3^-	^{i}Pr	Me	Me	−13.2	−12.8	−19.5	6.7
19	BF_3^-	^{i}Pr	CF_3	Me	−9.9	−10.0	−15.4	5.4
				^{n}Pr	−10.6	−11.1	−15.4	4.3
				CH(CN)Et	−3.8	−3.6	−15.5	11.9
20	BF_3^-	^{i}Pr	^{t}Bu	Me	−3.4	−4.6	−4.5	−0.1
				^{n}Pr	−2.7	−6.8	−4.6	−2.2
				CH(CN)Et	−4.6	−3.1	−11.3	8.2
21	SO_3^-	^{i}Pr	^{t}Bu	Me	0.2	−2.0	−1.1	−0.9
				^{n}Pr	−0.9	−4.5	−2.8	−1.7
				CH(CN)Et	3.0	1.4	−1.5	2.9
22	BF_3^-	BF_3^-	Me	Me	−15.0	−19.6	−18.4	−1.2
				^{n}Pr	−13.7	−16.0	−17.3	1.3
				CH(CN)Et	−9.2	−8.1	−17.0	8.9
23	BF_3^-	BF_3^-	CF_3	Me	−11.4	−9.7	−12.0	2.3
				^{n}Pr	−9.5	−5.3	−10.8	5.5
				CH(CN)Et	−3.8	0.5	−11.8	12.3
24	BF_3^-	BF_3^-	^{t}Bu	Me	−7.4	−11.8	−6.9	−4.9
				^{n}Pr	1.2	−8.2	−5.9	−2.3
				CH(CN)Et	−0.3	0.9	−10.3	11.2

linkages interacting with Ni have reduced bond orders compared to the noninteracting bonds. This can be rationalized by a back-donation type charge transfer from the occupied nickel d orbitals to the unoccupied π^* and σ^* orbitals of the B−F and S−O bonds. Coordination of ethylene or acrylonitrile to the metal weakens the Ni−F and Ni−O bond orders. Thus, ethylene or acrylonitrile coordination comes at the expense of Ni−F and Ni−O interactions. This explains why the complexation energies of ethylene and acrylonitrile are reduced considerably compared to the meta- and para-substituted species, where Ni−F and Ni−O interactions are absent. We note further that the Ni−F and Ni−O bond orders are reduced the most for the σ-complex, in line with the acrylonitrile complexation energy, which is weakened the most, resulting in the poisoning of **16** and **17** being eliminated. We have also examined the OBF_3^- substituent (**18**). It does not reduce the poisoning to the same degree, because the Ni−F bond is weaker.

The poisoning is not influenced a great deal by using either Me or *n*-propyl as the growing chain. However, for R = CH(CN)Et, the σ complexation is stabilized relative to π complexation due to the electron-withdrawing ability of the α-CN group, leading to an increase in the poisoning (Table 3).

Chart 7. Bond Orders of the Acrylonitrile and Ethylene π and σ Complexes of 16 and 17

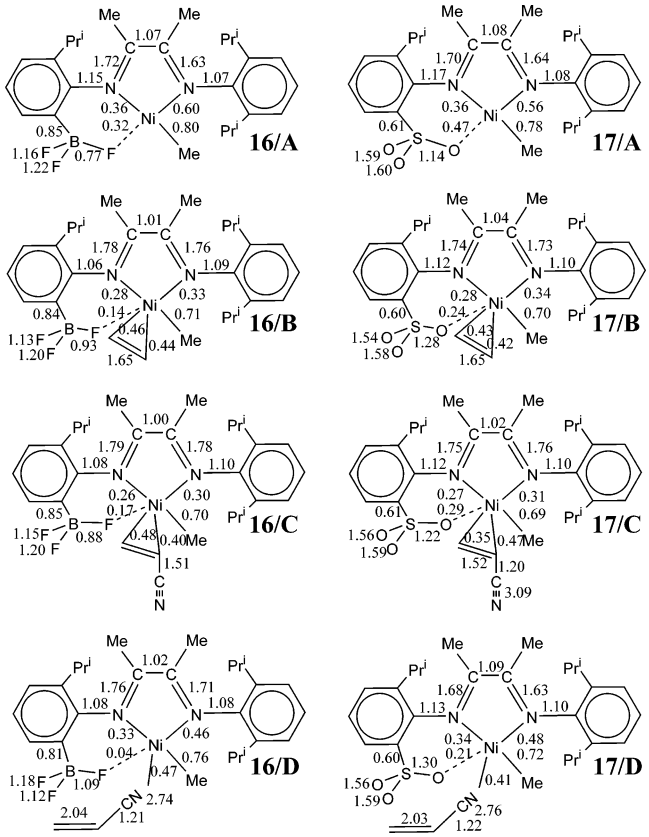

Combining Anionic Substitution on the Aryl Ring with Steric Bulk at the Diimine Backbone. We have also considered introducing steric bulk on the diimine backbone by replacing the methyl groups in the R_1 and R_2 positions by two electron-withdrawing CF_3 substituents (**19**) or two *t*-Bu groups (**20**) while maintaining one BF_3^- or SO_3^- substituent on one of the aryl rings. We find in accordance with the previous discussion regarding Chart 6 that the increase in steric bulk by pressing forward the aryl groups decreases both the π and σ complexation energies for all three systems (**19** and **20**). The bulk of the CF_3 is enough to push the aryl groups forward. However, it is not enough to prevent the aryl rotating from the perpendicular position in order to reduce the interaction with ethylene and AN. This helps especially AN in the σ mode, with the result that **19** is more poisoned than the complex **16**. The σ mode in **19** is also helped by the electron-withdrawing ability of CF_3.

The *t*-Bu at the backbone is sufficiently bulky to keep the aryl groups more upright, with the result that the degree of poisoning in **20** and **21** only differs marginally from that in the molecules **16** and **17**, as all three bonding modes are roughly destabilized to the same degree. As noted before for **16** and **17**, changing the growing chain in **19** and **20** from Me to *n*-propyl does not change the poisoning. However, the poisoning is increased by introducing CH(CN)Et, with an electron-withdrawing α-CN substituent.

Anionic Substitution on Each Aryl Ring To Produce an Anionic Diimine Ni(II) Complex. Addition of a second BF_3^- group to the unsubstituted aryl ring in **16**, **19**, and **20**, instead of an *i*-Pr group, gives

(38) Michalak, A.; DeKock, R. L.; Ziegler., T. Manuscript in preparation. The bond order method employed in this work is a modification of that published by Nalewajski and co-workers: (a) Nalewajski, R. F.; Mrozek, J. *Int. J. Quantum Chem.* **1994**, *51*, 187. (b) Nalewajski, R. F.; Mrozek, J.; Michalak, A. *Int. J. Quantum Chem.* **1997**, *61*, 589. (c) Nalewajski, R. F.; Mrozek, J.; Mazur, G. *Can. J. Chem.* **1996**, *74*, 1121. (d) Nalewajski, R. F.; Mrozek, J.; Michalak, A. *Polish J. Chem.* **1998**, *72*, 1779. (e) Michalak, A.; Ziegler, T. *Organometallics* **2003**, *22*, 2069.

Chart 8. Possible Anionic Substitutions on the Bridged Complex

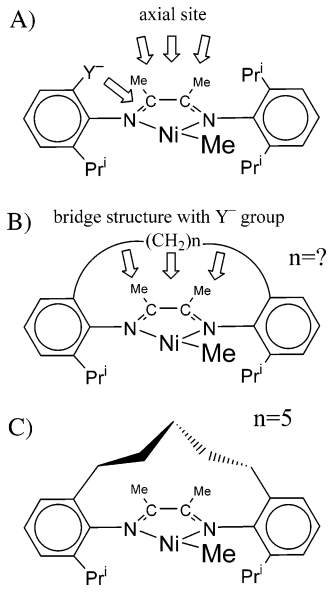

rise to the anionic species **22**−**24**, respectively. The two BF_3^- groups in the anionic species are not equivalent, in that one is more closely attached to the metal. The second BF_3^- substitution only results in minor changes in terms of both absolute bonding energies for ethylene and acrylonitrile and poisoning (Table 3). All of the aryl-substituted complexes **16**−**24** are promising in terms of poisoning. However, only **16**−**19**, **22**, **23** are real candidates if we also consider the criteria of $\Delta E_\pi < -5$ kcal mol^{-1}, unless these systems prove to have modest barriers of insertion ($\Delta E^\ddagger < 15$ kcal mol^{-1}).

Anionic Group Substituted Chain between the Two Aryl Groups. On the basis of our studies on the various backbone and aryl group substituted complexes, we believe that it is possible to promote the acrylonitrile π complex formation over the σ coordination. To find other effective places for the anionic group, we have carried out additional calculations for a modified Brookhart system.

In an earlier study by Deng et al., a very similar approach was used to boost the molecular weight in polymerization catalyzed by early-transition-metal complexes.[37] In our case, this bridge, shown in Chart 8, would provide a novel framework for the anionic substitution (Chart 8A,B).

On the basis of MM calculations we decided to use a pentylene chain, linking the two ends of the chain on the ortho carbon atoms of the aryl rings (Chart 8B). Using a chain shorter or longer than five CH_2 units would distort considerably the original diimine structure by bending the connecting aromatic carbon atoms out of the equatorial plane. The formally cationic complex, in Chart 8C and Figure 4, is the starting point for our further investigation. This structure contains at least three hydrogen atoms which can potentially be subjects for anionic substitution. The α-, β-, and γ-hydrogen atoms point toward the front side of the catalyst from the axial direction (Figure 4). Substituting these hydrogen atoms with anionic groups leads to new neutral catalyst candidates.

We have screened five different neutral bridge-type derivatives (**25**−**29**, Chart 4), to test the poisoning effect

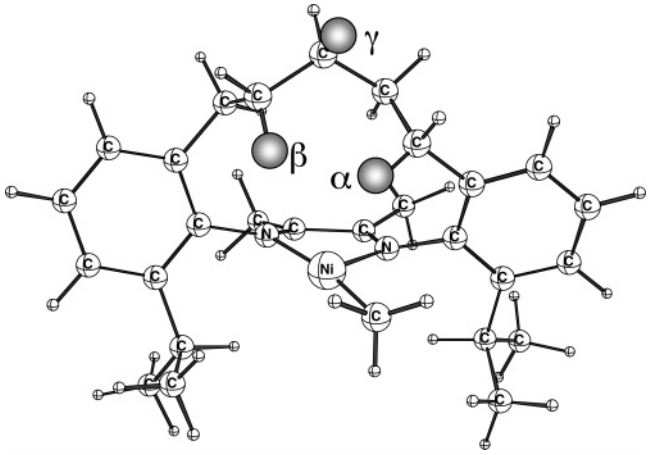

Figure 4. $(CH_2)_5$ bridge between the side (Ph) groups. Anionic substitution on the bridge at the α-, β-, and γ-hydrogen atoms.

Table 4. Relative Energies (kcal mol^{-1}) of the Ethylene and Acrylonitrile π and σ Complexes with Various Anionic Substitutions on the $(CH_2)_5$ Chain for the Bridge Type Complexes

ID	alkyl chain	anionic group	ET	AN		
			π	π	σ	$\pi-\sigma$
25	[Ni]−Me	γ-BF_3^-	−27.2	−26.2	−37.7	11.5
26	[Ni]−Me	γ-$CH_2BF_3^-$	−8.8	−9.0	−24.0	15.0
27	[Ni]−Me	γ-$(CH_2)_2BF_3^-$	−4.1	−5.6	−24.4	18.8
28	[Ni]−Me	β-BF_3^-	−18.9	−21.6	−26.0	4.4
28	[Ni]−^{n}Pr	β-BF_3^-	−9.4	−12.4	−17.3	4.9
28	[Ni]−CH(CN)Et	β-BF_3^-	−3.1	−8.6	−19.4	10.8
29	[Ni]−Me	α-BF_3^-	−6.0	−7.6	−10.7	3.1
29	[Ni]−^{n}Pr	α-BF_3^-	−3.8	−5.9	−9.4	3.5

of the polar CN group. On comparison of the σ and π complexation of acrylonitrile (Table 4), BF_3^- substitutions at the γ-carbon atom give rise to highly poisoned complexes. The γ-position is the most distant from the metal center; therefore, the anionic group cannot compete effectively with the polar group. Positioning the BF_3^- group closer to the Ni center, by growing an alkyl chain between the BF_3^- group and the γ-carbon atom, does not reduce the poisoning. This modification blocks the front side of the complex, therefore hindering the NC or double-bond coordination. Since π complexes are destabilized even more than σ complexes, the poisoning values increase for complexes **26** and **27** by 3.5 and 7.3 kcal mol^{-1}, respectively, with respect to that of complex **25**.

Substitutions on the α- and β-carbon atoms are more effective. The complexation energies of the β-BF_3-substituted σ- and π-acrylonitrile complexes (**28**) are considerably lower than for the α-BF_3-substituted complexes (**29**), indicating a sterically less bulky complex. However, the poisoning is slightly reduced for **29** compared to **28**; thus, our best bridge type candidate is still poisoned by 3.1 and 3.5 kcal mol^{-1} with the methyl and propyl chains, respectively. Of the bridged complexes **25**−**29,** the system **28** seems most promising in terms of P and ΔE_π.

Concluding Remarks

Polar olefinic monomers tend to poison olefin polymerization catalysts by bonding through their polar group (ΔE_σ) rather than through their π functionality (ΔE_π).

Thus, the classical cationic Ni(II) diimine complex, due to Brookhart, exhibits a preference of binding through the CN group of 22.0 kcal mol^{-1}. We have examined how the poisoning $P = \Delta E_\pi - \Delta E_\sigma$ can be reduced by anionic substitution on the classic Brookhart catalyst **0**. It is shown that the introduction of one or two anionic groups (BH_3^-, BF_3^-, SO_3^-, etc.) at the diimine backbone reduces the poisoning by up to 16 kcal mol^{-1} (**1**−**10**). An even larger reduction was found by substituting one (**13**−**18**) or two (**22**−**24**) *i*-Pr groups on the aryl rings, whereas substitution on other parts of the ring (**11** and **12**) is less effective.

An attempt at placing anionic groups on an alkyl chain connecting the two aryl rings was also effective in the β-position (**28**) but not in the α- and γ-positions (**25**−**27**, **29**).

An extensive analysis of the kinetics for propagation of acrylonitrile polymerization revealed that a good polar polymerization catalyst in addition to a low monomer insertion barrier and poisoning also must have a π−complexation energy between $\Delta E_\pi > -20$ and $\Delta E_\pi < -5$ kcal mol^{-1}. On the basis of this criteria we were able to select the most promising candidates of modified Ni(II)−diimine complexes for ethylene/acrylonitrile copolymerization. These candidates will be tested by calculating their barrier of ethylene and acrylonitrile insertion into the Ni−alkyl bond in a forthcoming investigation, where we will examine a few Pd(II) catalysts as well.

Acknowledgment. An important part of the calculations has been performed by the MACI cluster (Multimedia Advanced Computational Infrastructure) at the University of Calgary and by WestGrid computers. We thank Cheryl M. Abel for useful discussions and sharing her unpublished results with us. This work has been supported by the National Sciences and Engineering Research Council of Canada (NSERC), as well as Bayer Material Science and Lanxess. T.Z. thanks the Canadian government for a Canada Research Chair.

Supporting Information Available: Listings giving Cartesian coordinates of the various structures calculated in this paper. This material is available free of charge via the Internet at http://pubs.acs.org.

OM049018Z